

## Dynamics of counterpropagating pulses in photonic crystals: Enhancement and suppression of stimulated emission processes

M. Centini,<sup>1,2</sup> G. D'Aguanno,<sup>1,2</sup> M. Scalora,<sup>2</sup> M. J. Bloemer,<sup>2</sup> C. M. Bowden,<sup>2</sup> C. Sibilia,<sup>1</sup> N. Mattiucci,<sup>1</sup> and M. Bertolotti<sup>1</sup>

<sup>1</sup>*INFN at Dipartimento di Energetica, Università di Roma, "La Sapienza," Via A. Scarpa 16, I-00161 Rome, Italy*

<sup>2</sup>*Weapons Sciences Directorate, Research Development and Engineering Center, U.S. Army Aviation & Missile Command, Bldg. 7804, Redstone Arsenal, Alabama 35898-5000*

(Received 15 May 2002; revised manuscript received 18 December 2002; published 25 March 2003)

Using numerical methods, we study the propagation of counterpropagating pulses in finite photonic crystals. We show that linear interference and localization effects combine to either enhance or suppress stimulated emission processes, depending on the initial phase difference between the input pulses. We consider the example of second harmonic generation, where we find a maximum contrast of three orders of magnitude in nonlinear conversion efficiency as a function of the input phase difference between incident pulses. We interpret these results by viewing the photonic crystal as an open cavity, with a field-dependent, electromagnetic density of modes sensitive to initial and boundary conditions.

DOI: 10.1103/PhysRevE.67.036617

PACS number(s): 42.70.Qs, 42.79.Nv

We describe pulse propagation effects arising from the interaction between counterpropagating pulses in one-dimensional (1D) photonic crystals (PC's), under conditions of high field localization. The dynamics of counterpropagating pulses has been investigated and applied to colliding pulse mode locking in dyes [1], adiabatic pulse compression of solitons [2], and nonlinear loop mirrors [3], for example. Stimulated and spontaneous emission processes have also been studied for excited atoms and dipoles embedded in PC's [4,5,6]. However, the combined effects of interference and strong cavity feedback when pulses collide remain uninvestigated. The simultaneous presence of counterpropagating pulses creates unusual conditions that can lead to the control of stimulated processes, such as second harmonic generation, that depend on the initial phase difference between incident pulses. To be sure, coherent control of emission rates is not a new idea. In fact, it has previously been proposed to control phonon emission rates [7], final state population, ionization, and photodissociation in semiconductor materials [8], as well as the emission of terahertz radiation from semiconductor nanostructures [9].

Under these conditions, a density of states that depends only on internal material variables, i.e., a dispersion relation, no longer yields the correct stimulated emission rates. Later we will see that two counterpropagating pulses tuned to the same transmission resonance do not necessarily excite the cavity mode that one might expect at that frequency if the same pulses have an appropriate phase mismatch. As a result, the finiteness of the structure changes the nature of the problem to such an extent that the effective density of modes is dynamically modified enough to induce changes to stimulated emission rates. In other words, the dynamic density of modes is subject to initial and boundary conditions, with significant consequences when the linear dynamics is combined with gain or lossy materials, and/or nonlinearities, as we do here. In that case, one can envision novel devices such as phase-controlled optical delay lines, four-port optical switches, and colliding pulse mode lockers, to name a few.

We use numerical methods to study the dynamics of colliding pulses approximately 0.7 ps in duration. The calculations were carried out using a fast Fourier transform beam

propagation (FFT-BPM) method [10]. We consider a 12- $\mu\text{m}$  long, symmetric, 19 and  $\frac{1}{2}$  period PC composed of quarter-wave/half-wave layers with refractive indices that alternate between  $n_1=1$  and  $n_2=1.42857$ , respectively. For simplicity, we choose a reference wavelength of  $\lambda=1\ \mu\text{m}$ . Left-to-right (LTR) and right-to-left (RTL) propagating pulses are tuned to  $\lambda=1.69\ \mu\text{m}$ , where a  $\sim 5\text{-nm}$  band edge transmission resonance is found. The pulses are symmetrically located around the structure, and individually display a transmission of approximately 80% due to their finite bandwidth.

In Fig. 1 we depict the spatial distribution of typical incident [Fig. 1(a)] and scattered fields [Fig. 1(b)]. Reflected pulses are generally split into two main lobes. Transmitted pulses appear undistorted with respect to incident pulses, but with diminished intensity. Our calculations also show that there is a phase difference of  $\pi$  between the two lobes of the reflected field. The origin of this phase shift can be understood as follows: the approaching pulse probes the structure

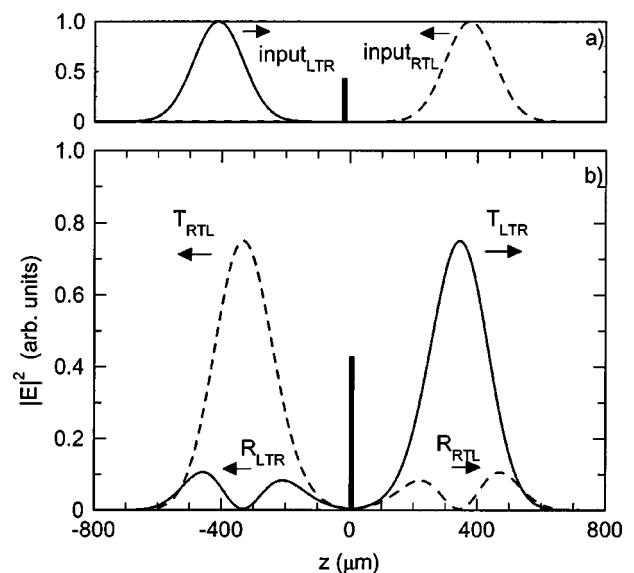


FIG. 1. Normalized input (a) and scattered (b) pulses propagating LTR (solid) and RTL (dashed). Pulse duration is approximately 0.7 ps.

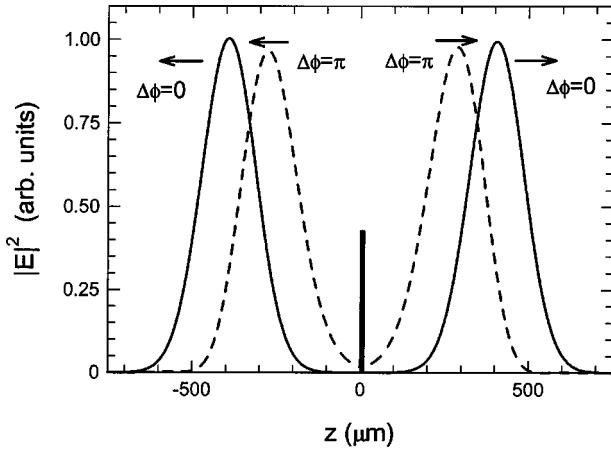


FIG. 2. Snapshots of outgoing pulses when input counterpropagating pulses have the relative phase difference  $\Delta\varphi=0$  (solid) and  $\Delta\varphi=\pi$  (dashed).

with its leading edge, and part of it is immediately reflected. This gives rise to a first reflected,  $\pi$  phase-shifted lobe, consistent with propagation from a low ( $n=1$ ) to a high index region ( $n=1.42857$ ). As the pulse continues on, the field is also in part reflected by the filtering effect of the structure, thus forming the second reflected lobe. At a peak of transmission, the total phase shift imparted to the transmitted field is an integer multiple of  $\pi$  [11]. It follows that upon reflection the second lobe is always phase shifted by twice as much, or an even multiple of  $\pi$ .

These preliminary observations are useful to understand the physics behind the interaction of counterpropagating pulses. We define the total field as

$$\begin{aligned} E(z,t) &= [\mathcal{E}_F(z,t)e^{ik_0z} + \mathcal{E}_B(z,t)e^{-ik_0z}]e^{-i\omega t} + c.c. \\ &= \mathcal{E}(z,t)e^{i(k_0z - \omega t)} + c.c.; \end{aligned} \quad (1)$$

$k_0$  is the vacuum wave vector and  $\mathcal{E}_F(z,t)$  and  $\mathcal{E}_B(z,t)$  are the LTR and RTL traveling pulse envelopes, respectively. We have also introduced a complex general field envelope  $\mathcal{E}(z,t)$ , which implicitly includes LTR and RTL components. Our initial condition at  $t=0$  for two identical Gaussian envelopes centered at  $z_1$  and  $z_2$ , can be written as

$$\mathcal{E}(z,0) = \mathcal{E}_0 \{ e^{(z-z_1)^2/2d^2} + e^{(z-z_2)^2/2d^2 + i(-2k_0z + \Delta\varphi)} \}. \quad (2)$$

$\Delta\varphi$  is the initial relative phase difference,  $d$  is the spatial width of the pulse, and its temporal duration is  $d = c\tau_{\text{FWHM}}/2\sqrt{\ln 2}$ , where  $c$  is the speed of light in vacuum. Our choice of initial wave-vector is consistent with pulses initially located in free space. All phase modulation effects that arise from multiple reflections, scattering, and nonlinear interactions are accounted for in the dynamics of the complex envelope [10].

In Fig. 2 we show the scattered, output fields for initial phase differences of 0 and  $\pi$ , respectively. The snapshots of the output pulses are taken at the same instant. Unlike their counterparts in Fig. 1, allowing the fields to interfere and become superimposed leads to what may at first appear as anomalous results: the group velocities of the output pulses

seem to be quite different. We conclude that, in a hypothetical experiment, pulses with an initial  $\Delta\varphi=0$  should be detected earlier compared to pulses with an initial  $\Delta\varphi=\pi$ .

This effect cannot be predicted *a priori*, or be explained in terms of interference of counterpropagating waves in a homogeneous medium because the solutions that we study are subject to specific initial and boundary conditions. In a homogeneous medium, a phase shift of  $\pi$  between counterpropagating pulses simply interchanges the location of light and dark fringes, and leaves the time of flight and directions of propagation of each field unaltered. In our case, the fields are the superposition of the reflected LTR (RTL) and the transmitted RTL (LTR) pulses depicted in Fig. 1. This yields a single RTL (or LTR) outgoing, smooth pulse—Fig. 2. We note that there is no way to predict *a priori* that outgoing pulses should be smooth or single peaked, given the nature of the superposition. Because the two reflected lobes of Fig. 1(b) have a relative phase shift of  $\pi$  with respect to each other, only one lobe can interfere constructively with the pulse transmitted from the opposite direction. The result is that the peaks of the outgoing pulses can appear to be pulled backward or pushed forward in space (and time), depending on the initial phase difference between incident pulses. While in Fig. 2 we have shown a case corresponding to extreme phase differences, the dynamics of intermediate phase values results in continuously tunable delays, as we will see below.

If we now look at the field distribution inside the structure during the interaction, we also find unusual field localization and pattern formation—Fig. 3. Snapshots are taken at the same instant in time for 0 [Fig. 3(a)],  $\pi$  [Fig. 3(b)], and  $\pi/4$  [Fig. 3(c)] phase shifts, when both peaks are inside the PC. In Fig. 3(a), which corresponds to the case of Fig. 2, there is nearly complete constructive interference: the energy is stored in the high index layers, a cavity mode is excited, and output pulses appear to be delayed more (Fig. 2). In fact, this is what one might expect due to localization effects at the band edge resonance, i.e., the mode excited is reminiscent of the cavity mode excited when light is incident from a single direction at that frequency. In Fig. 3(b), it seems as if the total electromagnetic field “interferes” itself out of the structure, in a mirrorlike interaction, with little or no penetration or delay, similar to what occurs to a wave tuned inside the gap. However, in all the cases that we refer to, once the fields enter the structure they become irrevocably intertwined, in the sense that a detector cannot distinguish on the original direction of propagation of any part of the pulse. The figure also leaves the impression that in Fig. 3(b) no field penetration occurs. In fact, each pulse still penetrates, becomes well localized inside the stack, and is transmitted or reflected regardless and independently of the other pulse, because in the linear regime there is nothing to couple them. Finally, in Fig. 3(c) yet another field distribution is depicted: the excited mode is not at all what one might expect when the incident field is tuned to the first transmission resonance. Therefore, we conclude that in the presence of multiple, counterpropagating pumping fields, pumping a finite structure at a given frequency is not enough to excite a cavity mode because the total field distribution is subject not only to boundary conditions, but also to initial conditions. Therefore, if one is to

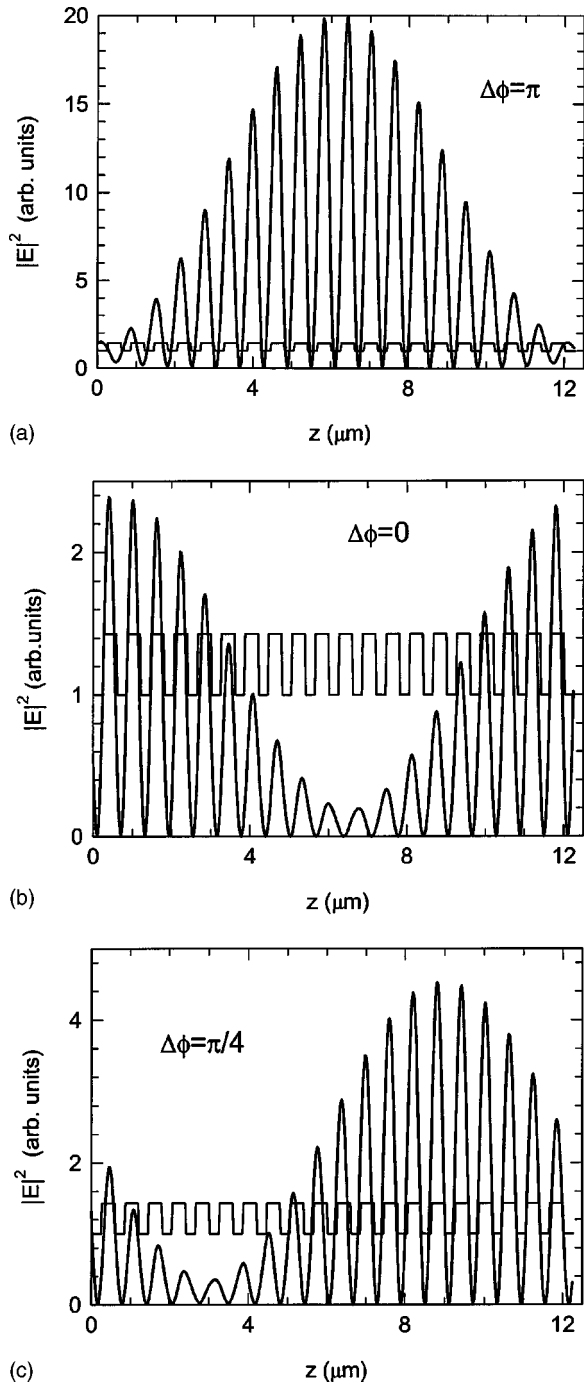


FIG. 3. Field intensity profiles inside the PBG, for  $\Delta\phi = \pi$  (a),  $\Delta\phi = 0$  (b),  $\Delta\phi = \pi/4$  (c) plotted against the index profile (thin solid curve). In all cases the peaks of both pulses have reached the structure, and the profile is very similar in shape and magnitude to the shape and profile of the mode generated by an incoming continuous wave.

associate field strength with a density of modes, this quantity must have the flexibility to adjust not only with respect to boundary conditions, but also with respect to initial conditions, which means that the effective density of modes should also be considered as a dynamics variable. We now suggest how to accomplish that.

In addition to the interferometric interpretation just ex-

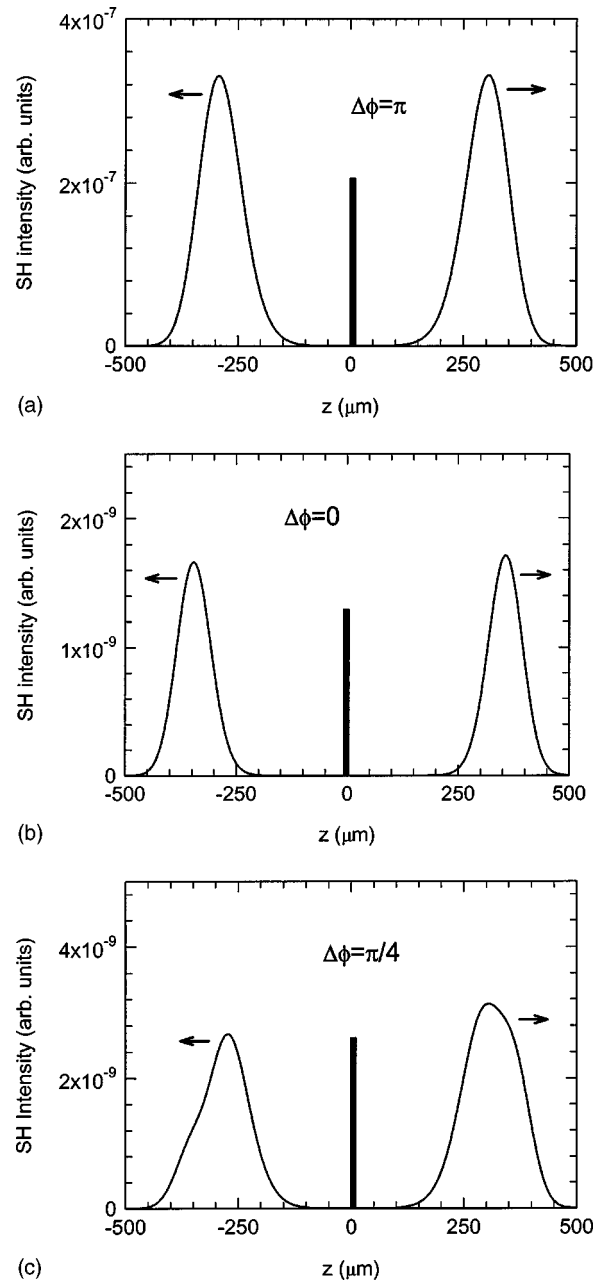


FIG. 4. Generated forward and backward SH pulses for  $\Delta\phi = \pi$  (a),  $\Delta\phi = 0$  (b),  $\Delta\phi = \pi/4$  (c), corresponding to the cases depicted in Fig. 3.

pounded, there is another way to approach this problem which in our view reveals the true complexion of open systems. For example, it is hardly appropriate to speak of a cavity mode for any structure coupled with the universe outside, or of a density of modes (DOM) that results only from a dispersion relation, without regard to the initial conditions. In Ref. [12] it is shown that the definition of a phase time  $\varphi_t$ , the phase of the transmitted field, can be used to define a density of modes (DOM) for a finite, 1D stack as

$$\rho_\omega = \frac{1}{L} \frac{d\varphi_t}{d\omega}. \quad (3)$$

Following a quantum mechanical analog, where the DOM is

proportional to the probability of finding a particle within a certain volume, in Ref. [13] a new definition of DOM emerged as the electromagnetic counterpart, namely [13],

$$\rho_\omega = \frac{1}{2Lc} \int_0^L \left( \varepsilon_\omega(z) |\Phi_\omega|^2 + \frac{c^2}{\omega^2} \left| \frac{d\Phi_\omega}{dz} \right|^2 \right) dz, \quad (4)$$

where  $L$  is the length of the structure and  $\Phi_\omega$  is the normalized electric field. While the equivalence of the electromagnetic DOM and the phase time DOM has not, to our knowledge, been established formally, it can be shown that the two are indistinguishable for a field incident from a single direction [13]. More importantly, unlike its phase-time counterpart, the electromagnetic DOM is explicitly dependent on the electric field, and hence clearly susceptible to boundary and initial conditions. The consequence is that by controlling field localization inside the stack (Fig. 3) one is able to control stimulated processes, e.g., the DOM. In our case, this is achieved coherently by manipulating the phase difference of the external excitation.

As an example of this, we analyzed second harmonic generation (SHG) by using a material with a nonzero  $\chi^{(2)}$  in the high index layers. By considering a typical amount of linear dispersion for the high index material, so that  $n_2(2\omega) = 1.52$ , using an effective index approach we are able to achieve a phase-matched interaction for the SH generation process [11]. In Fig. 4 we show SHG corresponding to the three pumping conditions of Fig. 3. When the mode profile is symmetric [(a) and (b) cases in both figures], SHG is also roughly symmetric. However, the case that corresponds to Fig. 3(c) yields an asymmetric SHG.

In Fig. 5 we show the predicted SHG efficiency and group delay of the pump fields (i.e., location of the peaks compared to two freely propagating input pulses) for RTL and LTR propagation as a function of the relative phase difference between the initial pulses. We find that the total SH conversion efficiency between the two extreme cases differs by three orders of magnitude. This curve also reflects the general characteristics of the electromagnetic DOM. Figure 5 also shows peculiar asymmetries in the RTL and LTR group delays. Maximum conversion efficiency is obtained when both interaction time and field localization are maximized [Fig. 3(a)], i.e., when the two curves intersect and when

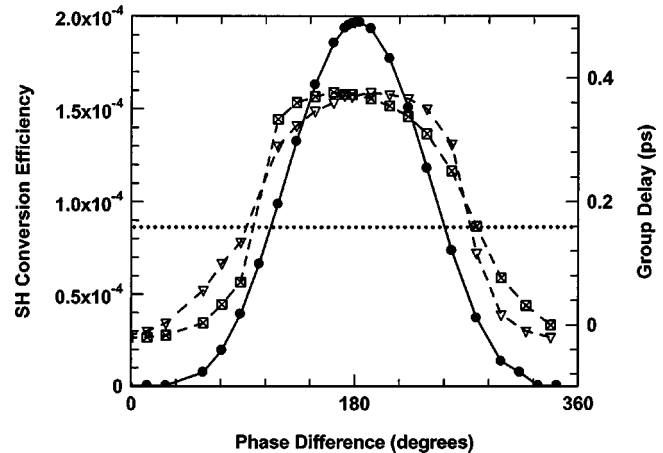


FIG. 5. Calculated second harmonic conversion efficiency (solid curve, solid circles), RTL (dashed curve, upside-down empty triangles), and LTR (dashed curve, crossed squares) group delays. With  $\chi^{(2)} \sim 80$  pm/V and peak field values of  $10^4$  V/m, the pump remains undepleted during the interaction, with conversion efficiencies that do not exceed  $10^{-6}$ . The flat, dotted line marks the constant group velocity for a RTL or LTR incident pulse with arbitrary phase.

$\Delta\varphi = \pi$ . The range of tunable delay oscillates between 0.4 ps and  $-10$ fs, indicating slightly superluminal group velocities. We note that the maximum group delay of individual LTR or RTL propagating pulses is phase independent and that for pulses 0.7 ps in duration it reaches a maximum of only 0.18 ps (dotted line in Fig. 5).

In summary, we have shown that there is a deeper physical interpretation of the DOM for open systems that goes beyond simple interference, which can affect dynamical variables such as group velocity and the efficiency of stimulated processes. We have shown that it is possible to control SHG conversion efficiency and modulate the group delay of pump fields by manipulating the phase difference between input, counterpropagating pulses. The theory can be extended to generic 1D structures, and we expect that similar effects will persist in multidimensional PC's.

M. Centini and G. D'Aguanno thank the U.S. Army and the Army Research Laboratory–European Research Office for partial financial support.

[1] R. Mentzel, *Photonics* (Springer-Verlag, Berlin, 2001).  
 [2] P. C. Reeves-Hall, S. A. E. Lewis, S. V. Chernikov, and J. R. Taylor, *IEEE Electron Device Lett.* **36**, 622 (2000).  
 [3] M. F. Arend, M. L. Dennis, I. N. Duling III, E. A. Golovchenko, A. N. Pilipetskii, and C. R. Menyuk, *Opt. Lett.* **22**, 886 (1997).  
 [4] M. Scalora, J. P. Dowling, M. D. Tocci, M. J. Bloemer, C. M. Bowden, and J. W. Haus, *Appl. Phys. B: Lasers Opt.* **60**, S57 (1995).  
 [5] M. D. Tocci, M. Scalora, M. J. Bloemer, J. P. Dowling, and C. M. Bowden, *Phys. Rev. A* **53**, 2799 (1996).  
 [6] M. Konôpka, *Phys. Rev. A* **60**, 4183 (1999).  
 [7] X. Hu and W. Pötz, *Phys. Rev. Lett.* **82**, 3116 (1999).

[8] R. J. Gordon, *Annu. Rev. Phys. Chem.* **48**, 595 (1997).  
 [9] W. Pötz, *Appl. Phys. Lett.* **72**, 3002 (1998).  
 [10] M. Scalora and M. E. Crenshaw, *Opt. Commun.* **108**, 191 (1994).  
 [11] M. Centini, C. Sibilìa, M. Scalora, G. D'Aguanno, M. Bertolotti, M. J. Bloemer, C. M. Bowden, and I. Nefedov, *Phys. Rev. E* **60**, 4891 (1999).  
 [12] J. M. Bendickson, J. P. Dowling, and M. Scalora, *Phys. Rev. E* **53**, 4107 (1996).  
 [13] G. D'Aguanno, M. Centini, M. Scalora, C. Sibilìa, M. J. Bloemer, C. M. Bowden, J. W. Haus, and M. Bertolotti, *Phys. Rev. E* **64**, 016609 (2001).